Resonant tunnelling lifetimes in multi-barrier structures - a complex coordinate approach

1996 J. Phys.: Condens. Matter 8 6393

(http://iopscience.iop.org/0953-8984/8/35/008)

J. Phys.: Condens. Matter **8** (1996) 6393–6403. Printed in the UK

Resonant tunnelling lifetimes in multi-barrier structures—a complex coordinate approach

M Bylicki, W Jaskólski and R Oszwałdowski
Instytut Fizyki UMK, Grudziądzka 5, 87-100 Toruń, Poland†

Received 3 January 1996, in final form 13 May 1996

Abstract. The complex coordinate approach, widely used in theoretical atomic spectroscopy, is applied here to study energies and lifetimes of resonant tunnelling in double-barrier heterostructures within an applied electric field. The method gives very accurate results and they are compared with those obtained by other methods. Possible applications of this method for studying resonant states in various low-dimensional structures are discussed.

1. Introduction

Resonant energy structure of quantum wells, double barriers, superlattices and quantum dots in electric fields has been for the last two decades a subject of intensive experimental and theoretical investigation [1–14]. This is because the resonant tunnelling leads to the observed effects of fast response time and negative differential resistance, which open up possibilities of building new high-frequency modulation devices.

The methods used to calculate tunnelling lifetimes in multibarrier structures (or decay times in the case of quantum wells) are usually based on the one-band effective-mass approximation. The time-independent methods can be divided into two groups. In the first [5, 6] the model potential that represents the multibarrier (or quantum well) structure is placed in a large infinite-potential well leading to discretization of the continuum energy spectrum. Among the exact (matching) or approximate (in a basis) solutions of the Schrödinger equation for such a system, there are few bound states that show a significant probability of finding an electron in the well regions. They correspond to metastable resonant states. In the other group of methods [3, 4, 9] one considers transmission of plane waves or Airy solutions and the knowledge of tunnelling lifetimes is derived from this analysis. In yet another method, the time-dependent Schrödinger equation is solved for wave packets scattered by the model potential [14].

In the descriptions mentioned above, both the energy and the tunnelling lifetime of a resonant state are depicted by graphs, on which some calculated quantities are plotted versus electron energy. In the method of Borondo and Sanchez-Dehesa [5] and of Porto *et al* [6], applied to quantum wells and double-barrier structures (DBS) in an electric field, respectively, the resonant energies E_r and widths Γ (tunnelling lifetime $\tau = \hbar/\Gamma$) are determined by the Fermi Golden Rule and taken from the stabilization graphs that show positions of bound states versus changing the size of a large infinite-potential well. In the method of Bloss [9] both E_r and Γ are read from the local density of states $\rho(E)$

† E-mail: wj@phys.uni.torun.pl.

0953-8984/96/356393+11$19.50

calculated using the relation $\rho = -(2/\pi)\mathrm{Im}\, G(E)$. Similarly, in the methods that analyse transmission and reflection of incoming waves, E_r and Γ are identified with the peaks in graphs of phase-shifts [4] or transmission coefficients [3]. In the time-dependent approach [14] the resonant energies are recognized as peaks in *I–V* characteristics and the tunnelling times are approximated by saturation times of the tunnelling probability. Although this method allows for tracing in time the process of resonant tunnelling, it is much more computer time and memory consuming than the standard stationary approaches.

One of the advantages of the complex coordinate rotation methods [15, 16] is that, as in the case of exact matching methods [10–12], one gets the complex energies $E_{res} = E_r - \mathrm{i}\Gamma/2$ of the resonant states directly. They are eigenvalues of the Hamiltonian matrix evaluated using normalizable functions and complex rotated coordinates, $x\mathrm{e}^{\mathrm{i}\theta}$, either in the Hamiltonian or in the basis functions. The complex eigenvalues form θ-trajectories on the complex plane. The resonances are identified with the θ-independent eigenvalues (for some range of the rotation angle θ). Methods of this kind are widely, and successfully, used in the investigations of atomic and molecular autodecaying states [15, 16]. For the present application we have chosen the method developed by Nicolaides and co-workers (see [16]) because of its simplicity and fast convergence property [17]. The standard, previously mentioned methods, that are based on the procedure of matching of the exact solutions of different structure regions, were originally designed for treating mainly one-dimensional rectangular multibarriers. Extension of these methods to other structures is neither simple nor straightforward. In contrast, the complex coordinate approach can be easily applied to quantum dots, to quantum wires, to any kind of profiled or doped structures and to multiband Hamiltonians, since it always consists in diagonalization of the Hamiltonian matrix performed for several values of the rotation angle θ.

In this work we present a preliminary application of the complex coordinate rotation method to the problem of resonant tunnelling in symmetrical DBS, that has been frequently used for testing various approaches [3–14]. We show here how stable this method is, even for high external electric fields applied, yielding accurate results for the resonance positions and lifetimes, in the minimal gaussian basis sets used. We also perform a study of the behaviour of energy positions and lifetimes of the ground and excited resonant states versus an applied electric field, for two different DBS. The method is briefly explained in the next section. The results of the application are presented in section 3.

2. Outline of the method

The problem that we deal with in this paper belongs to the class of non-stationary or resonance state problems. Such systems can be treated by methods involving the use of complex coordinates [15, 16]. We repeat here the most essential elements of the approach called the complex eigenvalue Schrödinger equation (CESE) as developed by Nicolaides and co-workers (see [16]).

The wave function of a system in the vicinity of the resonance (energy close to the resonance energy) can be written as

$$\Psi(x) = \psi_0(x) + \chi_{as}(x) \tag{2.1}$$

where ψ_0 stands for the localized part of the state, responsible for its quasistationary character, and χ_{as} is the unbound part of the state having an asymptotic behaviour appropriate to the case under consideration. The dynamics of the decay of the resonance is governed by the interaction between these two parts.

The wave function (2.1) contains all of the information about the system both *on* and *off* resonance. It satisfies the equation

$$(H - E)\Psi(x) = 0 \tag{2.2}$$

where H is the full Hamiltonian of the system. The energy E is a real number *off* the resonance. However, *on* resonance the asymptotic form of the wave function demands E to be a complex number with the imaginary part negative:

$$E_{res} = E_r - \frac{1}{2}\Gamma\mathrm{i}. \tag{2.3}$$

In the case of electric field potential resonances and short-range potentials (both closely related to our problem) this fact was discussed in detail by Nicolaides and Themelis [18] and Nicolaides, Komninos and Mercuris [19].

When considering the time-independent Schrödinger equation (2.2) for the resonance one assumes that the time evolution of the system is described by

$$\exp\left(-\mathrm{i}\frac{E_{res}}{\hbar}t\right) = \exp\left(-\mathrm{i}\frac{E_r}{\hbar}t\right)\exp\left(-\frac{\Gamma}{2\hbar}t\right) \tag{2.4}$$

and therefore the state decays exponentially with the lifetime $\tau = \hbar/\Gamma$.

The difficulty in solving the complex energy Schrödinger equation is that the proper boundary conditions must be imposed on the solution. However, this can be easily handled by transforming the spatial coordinate so that the resonant eigenfunction becomes bound, the Hamiltonian is non-Hermitian and the eigenvalue, i.e., the complex energy of the resonance, remains unchanged. There are several transformations which turn the unbound resonance function into the square-integrable function space [18]. The most commonly used one [15] is the complex rotation of coordinates

$$x \to x\mathrm{e}^{\mathrm{i}\theta} \tag{2.5}$$

(with real parameter θ) introduced by Dykhne and Chaplik [20] for the regularization of resonances of short-range potentials. This transformation was proven by Nicolaides and Themelis [18] to be computationally convenient with good convergence properties for both dc- and ac-field problems.

If one replaces x in χ_{as} of equation (2.1) by $x\mathrm{e}^{\mathrm{i}\theta}$ then the result

$$\tilde{\chi}_{as}(x) \equiv \chi_{as}(x\mathrm{e}^{\mathrm{i}\theta}) \tag{2.6}$$

is a square-integrable function of x, providing that θ is in the proper range, $\theta \in R_\theta$, depending on the asymptotic form of $\chi_{as}(x)$ (e.g. $0 < \theta < \frac{3}{2}\pi$ for the LoSurdo–Stark problem [18]). Therefore $\tilde{\chi}_{as}(x)$ can be expressed as an expansion

$$\tilde{\chi}_{as}(x) = \sum_{k=1}^{\infty}\phi_k(x) \tag{2.7}$$

in a complete basis set of square-integrable functions ϕ_k. Back rotation (replacing $x\mathrm{e}^{\mathrm{i}\theta}$ by x) gives

$$\chi_{as}(x) = \tilde{\chi}_{as}(x\mathrm{e}^{-\mathrm{i}\theta}) = \sum_{k=1}^{\infty}\phi_k(x\mathrm{e}^{-\mathrm{i}\theta}). \tag{2.8}$$

It should be emphasized that equation (2.8) is strict and $\chi(x)$ does not depend on θ under the condition that $\theta \in R_\theta$.

In practice, finite basis sets are used to represent χ_{as}. The localized part of the wave function, ψ_0, is also represented in a basis of square-integrable functions. Hence the

problem of solving equation (2.2) for the resonance energy and wave function is reduced to a variational problem in a basis of square-integrable functions. One part of the basis, chosen to represent the localized part of the resonance, is taken as functions of just x. The other part of the basis consists of functions of $x\mathrm{e}^{-\mathrm{i}\theta}$ so as to describe χ_{as}. The variational procedure leads to the Hamiltonian matrix eigenproblem (generalized if the basis is non-orthonormal). Since the basis functions are square-integrable [21] all of the matrix elements are finite and, in principle, there is no problem with their evaluation.

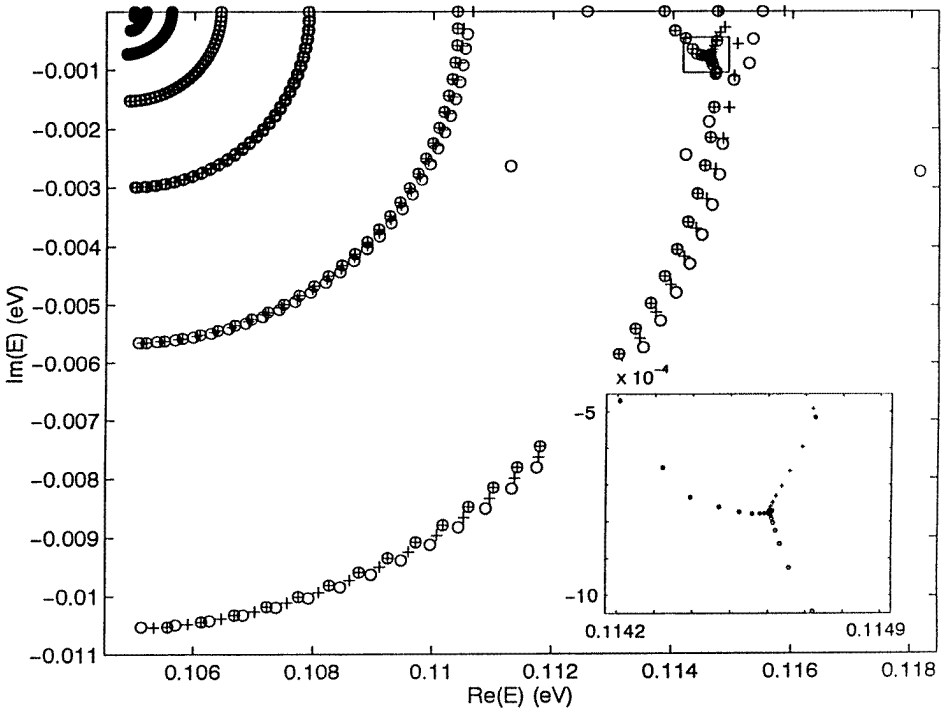

Figure 1. The θ-trajectories formed by the eigenvalues obtained for three slightly different basis sets (+, ○, ⊕) for the 40–60–40 DBS in the $F = 0.0015$ eV Å^{-1} electric field. All of the θ-trajectories start at the real axis for $\theta = 0$. Each trajectory consists of 30 points corresponding to uniformly distributed values of θ in the range from 0 to $\pi/4$. The eigenvalues corresponding to unbound states are homogeneously placed along the θ-trajectories. For a given θ they lie on a half-line rotated (approximately) by the angle 2θ into the lower complex half-plane, around the continuum threshold point (0.105 eV for $F = 0.0015$ eV Å^{-1}). The θ-trajectories corresponding to the resonance converge to a well determined point independent of the basis set (see the inset where the vicinity of the convergence point is magnified) though the starting points at $\theta = 0$ differ much more than for the unbound-state θ-trajectories.

The Hamiltonian matrix is complex and symmetrical. So it is non-Hermitian and its eigenvalues are complex. Some of them correspond to the resonances. If the basis set were complete it would be very easy to identify them. Since, in such a case, χ_{as} does not change with respect to variation of θ over its range R_θ, then the resonance eigenvalues also should be invariant. Truncation of the expansion (2.8) causes the basis set that is actually used to be better for some values of θ than for some others. Thus, the truncated expansion changes together with θ and so do the roots corresponding to the resonances.

Therefore, θ should be treated as an extra variational parameter. Diagonalization of the Hamiltonian is performed for several equidistant values of θ in the proper interval R_θ. Only those eigenvalues which stabilize against variation of θ should be considered as being approximate complex energies of resonances. The behaviour of the eigenvalues with respect to the variation of θ is shown in figure 1, for one of the systems investigated in this work. Considering the so-called θ-trajectories one can easily distinguish between the resonance eigenvalue and those corresponding to completely unbound states.

Table 1. Tunnelling lifetimes τ of the resonances in the double-barrier structures (a), (b) and (c) investigated for different applied bias $F(a+2b)$. A comparison with the results from other methods (see the text) is given. Parameters: m^*—effective mass; a—well width (Å); b—barrier width (Å); V_0—barrier height (eV).

		(a)			(b)			(c)	
m^*		0.41			0.41			0.67	
a		60			60			50	
b		40			70			50	
V_0		0.5			0.5			0.23	
Bias (meV)	n	CESE	SM	TC	CESE	SM	TC	CESE	MF
0	1	0.540	0.538	0.539	26.0	25.2	25.3	0.641	0.64
	2	0.025 36	—	—	0.197	—	—		
40	1	0.535	0.536	0.533	25.5	24.6	24.7		
	2	0.025 27	—	—	0.192	—	—		
100	1	0.507	0.504	0.506	22.9	22.0	22.2		
	2	0.024 75	—	—	0.173	—	—		

3. Results and discussion

In order to illustrate how the CESE method works for the problems of resonant tunnelling in semiconductor structures, we have applied it for studying the energy positions and widths of the resonant states in several symmetrical double-barrier structures. The DBS consist of two barrier material layers of thickness b separated by a thin well layer (thickness a) and placed between two thick well-type material layers. We work within the one-band effective-mass approximation and we consider the electron states only. The parameters of the DBS investigated are collected together in table 1. The columns (a) and (b) of the table correspond to the DBS based on $Ga_{0.47}In_{0.53}As/Al_{0.48}In_{0.52}As$ materials [6] while row (c) describes the $Ga_{0.75}Al_{0.25}As/GaAs$ structure [5]. For simplicity and for comparison with the results obtained by other methods we consider the effective mass as homogeneous over the whole DBS†. Since the barrier material is of high resistivity and since we assume the n-type materials to be in the outside regions, the potential outside the barriers is flat and the electric bias is applied only along the barrier well part of the DBS (see the inset in figure 2).

Because of the symmetry of the DBS the origin of the coordinate axis, $x = 0$, has been put in the middle of the well. The basis set has been chosen as $N = N_1 + N_2$ gaussian functions of even parity, $\phi_i = \exp(-\alpha_i x^2)$, and $M = M_1 + M_2$ odd-parity functions of the

† The effective mass enters into the Hamiltonian matrix through the kinetic energy integrals that for homogeneous m^* are evaluated analytically. One could use different m^* in different regions of DBS, but this would require one to calculate these integrals numerically. In addition it would be inconsistent with the usage of gaussian basis functions having their first derivatives continuous across the interfaces.

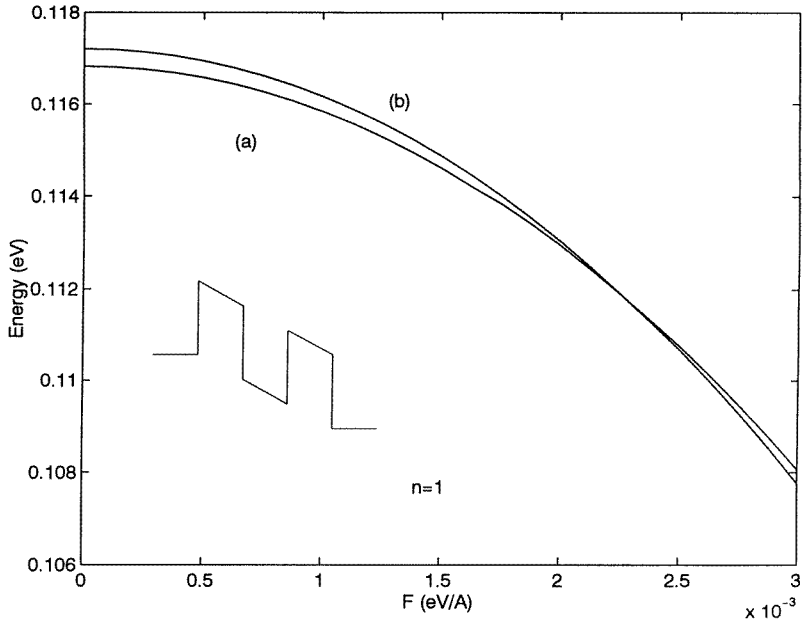

Figure 2. The dependence of the $n = 1$ resonance energy position, in eV, on the applied field F, in eV Å^{-1}, for the 40–60–40 DBS (a) and for the 70–60–70 DBS (b) of $Ga_{0.47}In_{0.53}As/Al_{0.48}In_{0.55}As$.

type $\phi_i = x\exp(-\alpha_i x^2)$. Using the non-orthogonal basis sets we are free to choose them as appropriate just from the structure geometrical point of view (determination of the initial exponents α_i). The non-orthogonality would anyway appear after the complex rotation of the coordinate even if we used an originally orthogonal basis. The N_2 even functions and M_2 odd functions have been rotated into the complex plane via the variable transformation $x \to x\mathrm{e}^{-\mathrm{i}\theta}$ (see equation (2.8)). The non-linear parameters α_i for all four function types (even-parity non-rotated, odd-parity non-rotated, even-parity rotated and odd-parity rotated) have been chosen as the even-tempered sets i.e., $\alpha_i = \alpha_0 q^i$. The exponents of the basis functions in each subset are thus defined by only two parameters, α_0 and q, and finally we end up with eight free parameters for each DBS. The parameters have been optimized (once for all the electric fields applied) in order to give the most stable and convergent θ-trajectories. In the case of structures (a) and (b), $N_1 = 22, N_2 = 13, M_1 = 22, M_2 = 13$, while for the DBS (c), $N_1 = 20, N_2 = 12$ (for this structure we present here only the field-free result for the only even-parity resonance).

The calculations have been performed for different values of the electric field eF changing from 0 to 3×10^5 eV cm^{-1}. The results are collected together in several figures showing clearly the behaviour of the energy positions and lifetimes of various resonances in different asymmetric DBS over the whole range of the applied field. The ground and first excited resonance energy positions (in eV), versus the electric field F, are presented in figures 2 and 3, respectively. The corresponding tunnelling lifetimes (in ps) are shown in figures 4 and 5. The lifetimes for some particular values of the electric field are presented in table 1 and are compared with the results obtained by the stabilization method (SM) [6], transmission coefficient analysis (TC) [6] and wave-function-matching method (FM)

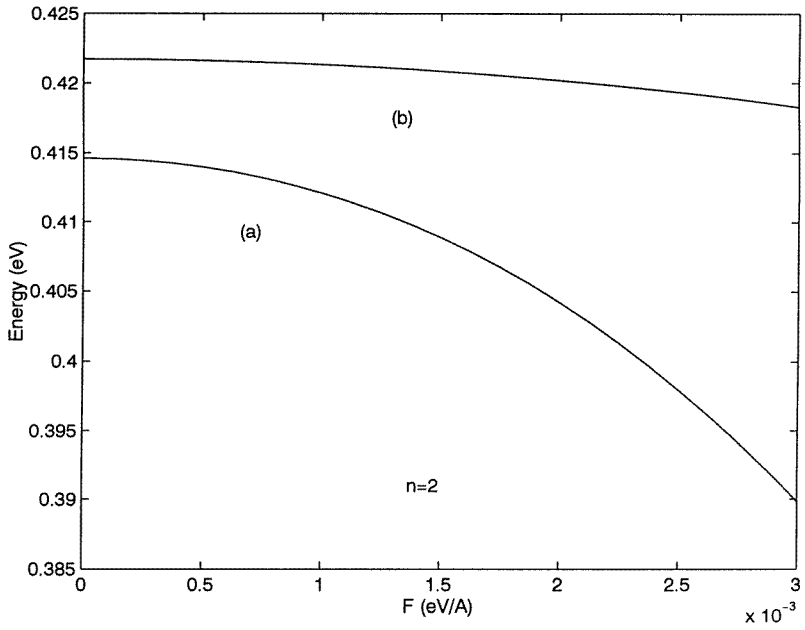

Figure 3. The same as in figure 2 but for the $n = 2$ resonance state.

[10]. It has been checked that the increase of the number of basis functions does not affect the significant figures of the results presented in table 1. Figure 6 shows additionally the convergence of θ-trajectories for the ground resonant state for a few different values of the field parameter F.

The lifetimes of the ground resonance state calculated using the CESE method are in very good agreement with the results obtained by other methods. However, it is significant that working with a single and not extensive basis set we were able to get stable and accurate results for higher resonances appearing below and above the barriers, and for higher fields than those usually investigated in the literature.

Let us now examine briefly some details of the results obtained. From figure 2 we can see that the shift (caused by the electric field) of the energy position of the lower ($n = 1$) resonant state is similar for both DBS, which differ in the barrier width.

However, for the second ($n = 2$) resonant state (figure 3) the energy position of this state for a 40–60–40 DBS goes down rapidly with the applied electric field, while it remains nearly unchanged in the case of a 70–60–70 DBS. This can be explained in terms of interaction with the continuum. In this case the excited resonance of the thicker structure lies energetically higher (closer to the top of the barrier) and already for low fields is strongly coupled to the continuum through the upper triangular part of the right-hand-side barrier (for $F \geqslant 0.8$ eV Å^{-1}, E_r is greater than the right-hand top of this barrier, and for $F \geqslant 2.7$ eV Å^{-1}, E_r is greater than the highest barrier top). This causes a fast *washing out* of this state from the well and the further increase of the field does not change the position of the resonance significantly.

The dependence of tunnelling lifetimes on the applied electric bias is, for both (a) and (b) structures and $n = 1, 2$ resonances, shown in figures 4 and 5. For $F \approx 0$ the τ in the DBS having thicker barriers are, as expected, much greater than the corresponding τ in the

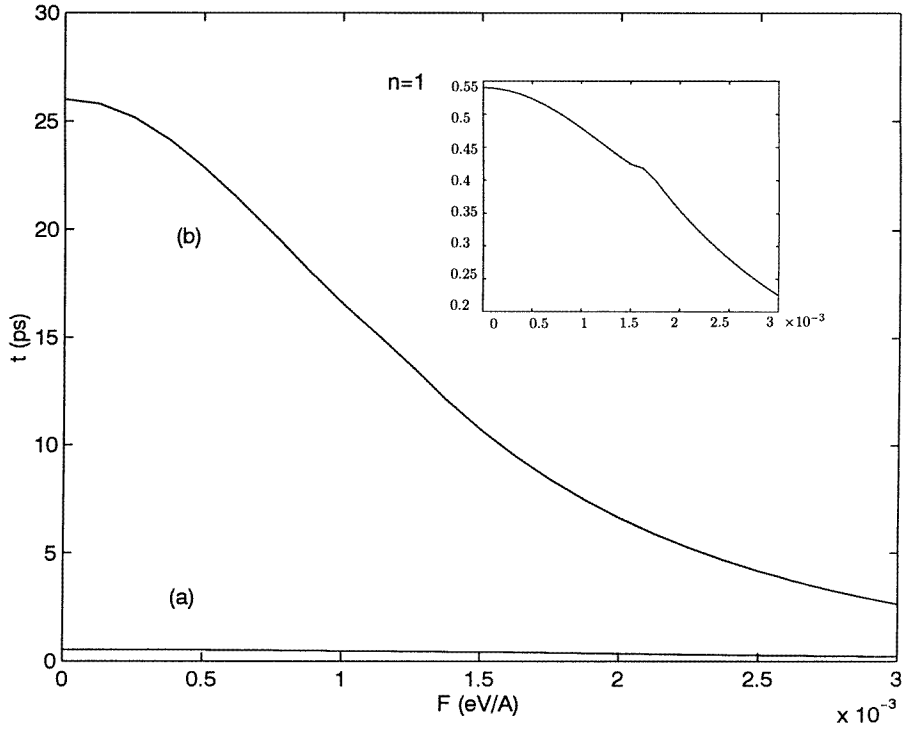

Figure 4. Tunnelling lifetimes, in ps, of the $n = 1$ resonance in the 40–60–40 (a) and 70–60–70 (b) DBS versus the applied electric field, in eV Å^{-1}.

thinner structure. Although the character of the $\tau(F)$-dependence, shown in the inset in figure 4, is similar for both DBS, the lifetime in the 70–60–70 DBS decreases much more rapidly with the field (by an order of magnitude) than for the 40–60–40 structure. This is because the resonant state in the latter structure is already for $F = 0$ much more diffuse (less stable) than the corresponding resonance in the former DBS. The decay channel opened up by the field plays thus a greater role in the broadening of the resonance in 40–60–40 DBS. For very high fields ($F \geqslant 3$ eV Å^{-1}) $\tau_{(b)}$ nearly reaches the value of $\tau_{(a)}$. This means that for the high-field regime the lifetimes are determined mainly by the field broadening of the resonant states.

For $F \geqslant 1.6$ eV Å^{-1} in the case of the 40–60–40 DBS and for $F \geqslant 1.2$ eV Å^{-1} for the 70–60–70 DBS, the ground resonance becomes a quasibound well state (its energy lies below the left-hand-side potential edge and τ corresponds now to the decay time). This fact is most clearly reflected in the structure of $\tau_{(a)}(F)$ shown in the inset of figure 4.

The results presented show the usefulness of the CESE method in studying resonant tunnelling phenomena in multibarrier structures. Working with the very limited gaussian basis sets and with only a few optimized non-linear parameters we were able to obtain stable and accurate results for energy positions and lifetimes for different structures and for high applied electric fields. The method is undoubtedly less computer time consuming than the other standard approaches, in which interface matching or integration of the Schrödinger equation has to be performed for a large number of energies in order to correctly reproduce the character of the transmission coefficient curve for all of the resonances. In the complex

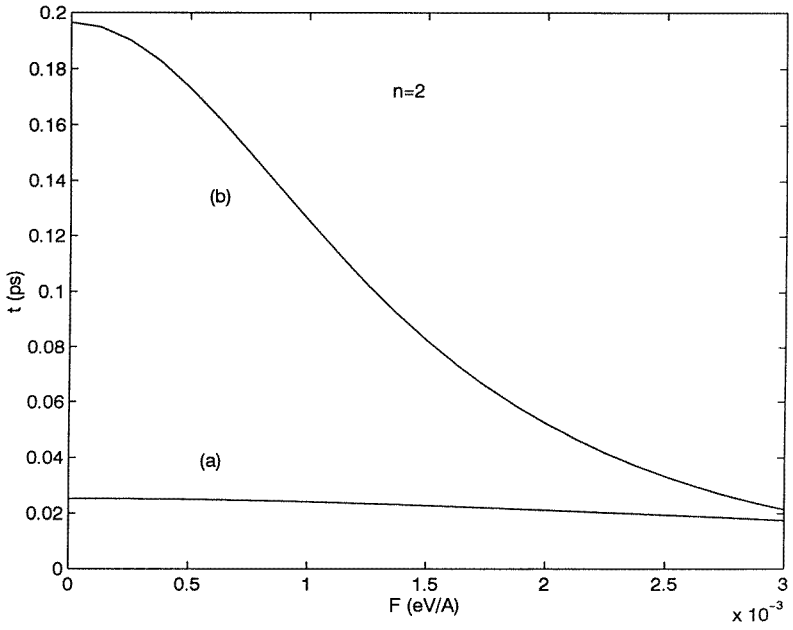

Figure 5. The same as in figure 4 but for the $n = 2$ resonance state.

coordinate approach, usually 15 values of θ are sufficient to get correct energy positions and widths of all of the resonances appearing in the structure investigated. The only weak point of this method is that it requires one to perform several initial calculations for checking stability and convergence of the basis functions.

Apart from giving a test illustration of the application of the complex coordinate rotation method to the problems of resonant tunnelling in semiconductor low-dimensional structures, we have also investigated the behaviour of various resonant states in different symmetrical DBS versus an applied electric field. We have shown that the method allows one to investigate also higher resonances—even those that appear above the barrier. It thus constitutes a useful tool for the investigation of energy structure of other low-dimensional systems. We mean here, for instance, resonant states of donors or excitons confined in quantum wells and quantum wires. Basis set calculations of the discrete energy structure of such systems are frequently performed [22]. Extension to the investigation of resonant states of these systems is, in terms of the complex rotation method, straightforward. Another example is the resonant tunnelling states of Coulomb island or quantum dots. Their spherical models are similar to those of atoms, for which the complex rotation method has been most widely used in the investigation of resonant states. Application of this method to the study of resonances in quantum dots is already in progress. The method should also be easily applicable to finding the resonant energy structure of on-the-surface absorbed atoms [23], which is important for an understanding of scanning tunnelling spectroscopy phenomena.

Acknowledgment

Support from KBN project No 2 PO3B 156 10 is gratefully acknowledged.

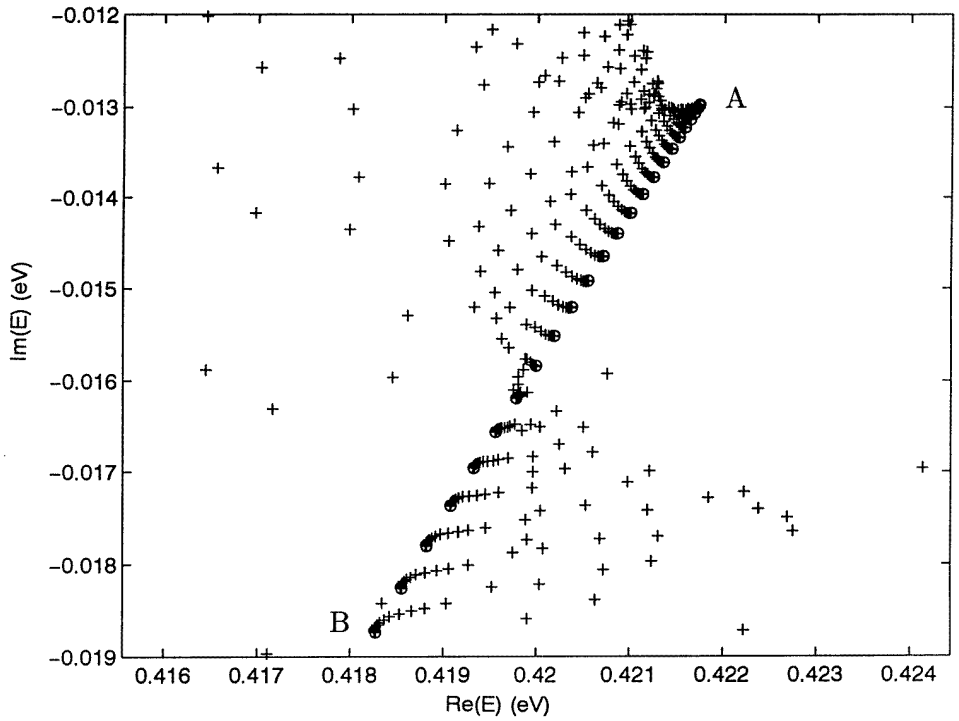

Figure 6. The convergence of θ-trajectories for the $n = 2$ resonance in the 70–60–70 DBS for 25 equidistant field values from $F = 0$ eV Å^{-1} (point A) to $F = 0.003$ eV Å^{-1} (point B). Each trajectory consists of 40 points marked as $+$. Some of them, those for the first 5–10 small values of θ, may seem to be distributed in a chaotic way. However, for larger θ-values the θ-trajectories are clearly distinguishable. The optimal points on each trajectory are marked by $\bigcirc$.

References

[1] Tsuchiya M and Sakaki H 1986 *Japan. J. Appl. Phys.* **25** L185
[2] Hauge E H and Stonvneng J A 1989 *Rev. Mod. Phys.* **61** 917
[3] Tsu R and Esaki L 1973 *Appl. Phys. Lett.* **22** 562
Price P J 1988 *Phys. Rev.* B **38** 1994
[4] Austin E J and Jaros M 1985 *Phys. Rev.* B **31** 5569
[5] Borondo F and Sanchez-Dehesa J 1986 *Phys. Rev.* B **33** 8758
[6] Porto J A, Sanchez-Dehesa J, Cury L A, Nogaret A and Portal J C 1994 *J. Phys.: Condens. Matter* **6** 887
[7] Bastard G 1988 *Interfaces, Quantum Wells, and Superlattices* (New York: Plenum) p 189
[8] Mendez E E 1988 *Interfaces, Quantum Wells and Superlattices* (New York: Plenum) p 227
[9] Bloss W 1989 *J. Appl. Phys.* **66** 1240
[10] Bahder T B, Morrison C A and Bruno J D 1987 *Appl. Phys. Lett.* **51** 1089
[11] Ahn D and Chuang S L 1986 *Phys. Rev.* B **34** 9034
[12] Peng J P, Chen H and Zhou S X 1991 *Phys. Rev.* B **43** 12 042
[13] Bryant G W 1989 *Phys. Rev.* B **39** 3145
[14] Bała P and Bała W 1995 *Appl. Phys.* A **60** 293
[15] See the issue on complex scaling:
Int. J. Quantum Chem. 1978 **14** No 4
and see also
Reinhart W P 1982 *Annu. Rev. Phys. Chem.* **33** 223
Ho Y K 1983 *Phys. Rep.* **99** 1

Bylicki M, Themelis S I and Nicolaides C A 1994 *J. Phys. B: At. Mol. Phys.* **27** 2741

[16] For references see
Nicolaides C A 1992 *Applied Many-Body Methods in Spectroscopy and Electronic Structure* ed D Mukherjee (New York: Plenum) p 233

[17] Bylicki M and Nicolaides C A 1993 *Phys. Rev.* A **48** 3589

[18] Nicolaides C A and Themelis S I 1992 *Phys. Rev* A **45** 349

[19] Nicolaides C A, Komninos Y and Merkuris T 1981 *Int. J. Quantum Chem.* S **15** 355

[20] Dykhne A M and Chaplik A V 1961 *Zh. Eksp. Teor. Fiz.* **40** 1427 (Engl. Transl. 1961 *Sov. Phys.–JETP* **13** 1002)

[21] In the expansion (2.7) we use the square-integrable functions $\phi_k(x)$. After the back-rotation transformation $x \to x\mathrm{e}^{-\mathrm{i}\theta}$ they may become unbound functions of x. Nevertheless the basis set used in practice, e.g., the Slater-type orbitals or the gaussian-type functions, remain the square-integrable functions of x even after the back rotation, provided that θ is in an appropriate range. This computational advantage has a less advantageous side: $\chi_{as}(x)$ does not vanish at infinity, so the finite representation in the square-integrable basis is not satisfactory from a formal point of view. However, this influences the accuracy of the energy computation very little, because within such a basis one can represent accurately enough the most important part of χ_{as}, i.e., the part in the finite spatial region where it interacts with the localized part of the state Ψ_0.

[22] Jaskólski W 1996 *Phys. Rep.* **271** 1

[23] Maniv T, Engdahl E and Moiseyev N 1987 *J. Chem. Phys.* **86** 1048